

Presented at the "3rd  
Intern. Conf. on Cluste  
ring Aspects of Nuclear  
Structure and Nuclear  
Reactions", Winnipeg

ISTITUTO NAZIONALE DI FISICA NUCLEARE  
Laboratori Nazionali di Frascati

LNF-78/28(P)  
27 Giugno 1978

F. Balestra, M. P. Bussa, L. Busso, I. V. Falomkin, R. Garfagnini,  
C. Guaraldo, A. Maggiora, G. Piragino, G. B. Pontecorvo, Yu. A.  
Shcherbakov, R. Scrimaglio and A. Zanini: CLUSTERING  
EFFECTS IN THE PHOTODISINTEGRATION OF  $^4\text{He}$  AND  
IN THE  $(\pi^+, ^4\text{He})$  ABSORPTION REACTIONS.

F. Balestra<sup>(x)</sup>, M. P. Bussa<sup>(x)</sup>, L. Busso<sup>(x)</sup>, I. V. Falomkin<sup>(o)</sup>, R. Garfagnini<sup>(x)</sup>, C. Guaraldo, A. Maggiora, G. Piragino<sup>(x)</sup>, G. B. Pontecorvo<sup>(o)</sup>, Yu. A. Shcherbakov<sup>(o)</sup>, R. Scrimaglio and A. Zanini<sup>(x)</sup>: CLUSTERING EFFECTS IN THE PHOTODISINTEGRATION OF  $^4\text{He}$  AND IN THE  $(\pi^+, ^4\text{He})$  ABSORPTION REACTIONS.

(Contributed paper presented at the "3rd International Conference on Clustering Aspects of Nuclear Structure and Nuclear Reactions" - Winnipeg, June 19-23, 1978).

The total and differential cross-sections, the angular and energy correlations for the three- and four-bodies  $^4\text{He}$  photodisintegration have been investigated, with a diffusion cloud-chamber placed in a magnetic field and exposed to the 100 MeV electrosynchrotron of Torino University<sup>(1,2)</sup>. In Fig. 1 the behaviour of the  $(\gamma, pn)$  cross-section is shown in the  $28 \leq E_\gamma \leq 60$  MeV interval. As one can see, the results are in rather good agreement with the older experimental data of Gorbunov<sup>(3)</sup> and of Arkatov et al.<sup>(4)</sup> and with the calculations of Dzhibuti et al.<sup>(5)</sup> and of Naguchi and Prats<sup>(6)</sup>, performed on the basis of the quasideuteron mechanism in the photodisintegration of  $^4\text{He}$ . The position of the maximum is better reproduced by the calculations of Naguchi and Prats.

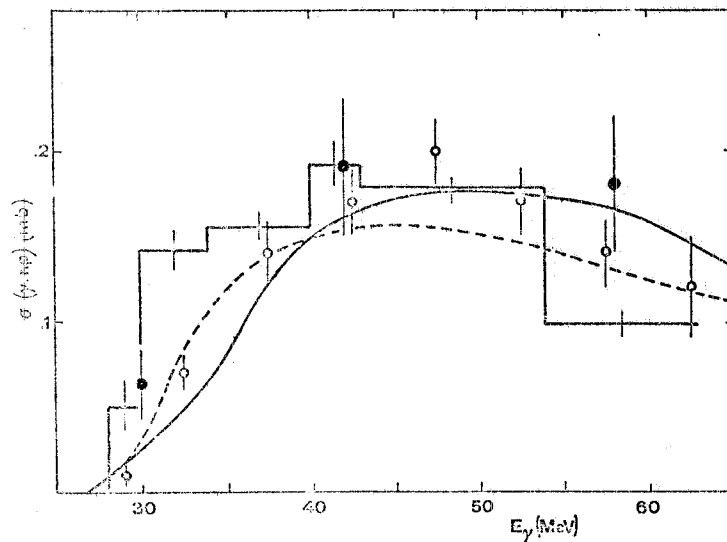


FIG. 1 -  $^4\text{He}(\gamma, pn)^2\text{H}$  reaction cross-section. Full line histogram: present work; full points: ref. (3); open circles: ref. (4); full line curve: ref. (5); dashed line curve: ref. (6).

(x) Istituto di Fisica dell'Università di Torino, and INFN, Sezione di Torino.  
(o) JINR, Dubna (USSR).

To better analyze the experimental data, the events have been grouped in two energy intervals, for  $28 \leq E_\gamma \leq 40$  MeV and for  $40 < E_\gamma < 60$  MeV. In Fig. 2 the distributions of the events as a function of the opening angle between the n-p, p-d and n-d pairs, are shown. The dashed histograms represent the distribution of the events with  $\theta_{np} > 90^\circ$  (about 71% of the total), that is of the events with presumable photon absorption by a n-p pairs. It is interesting to note that the events with  $E_\gamma > 40$  MeV and  $\theta_{np} \leq 90^\circ$  (about 15% of the total) have the neutron and deuteron emitted with large opening angle, that is with presumable photon absorption by a n-d pair. In Fig. 3 the relative

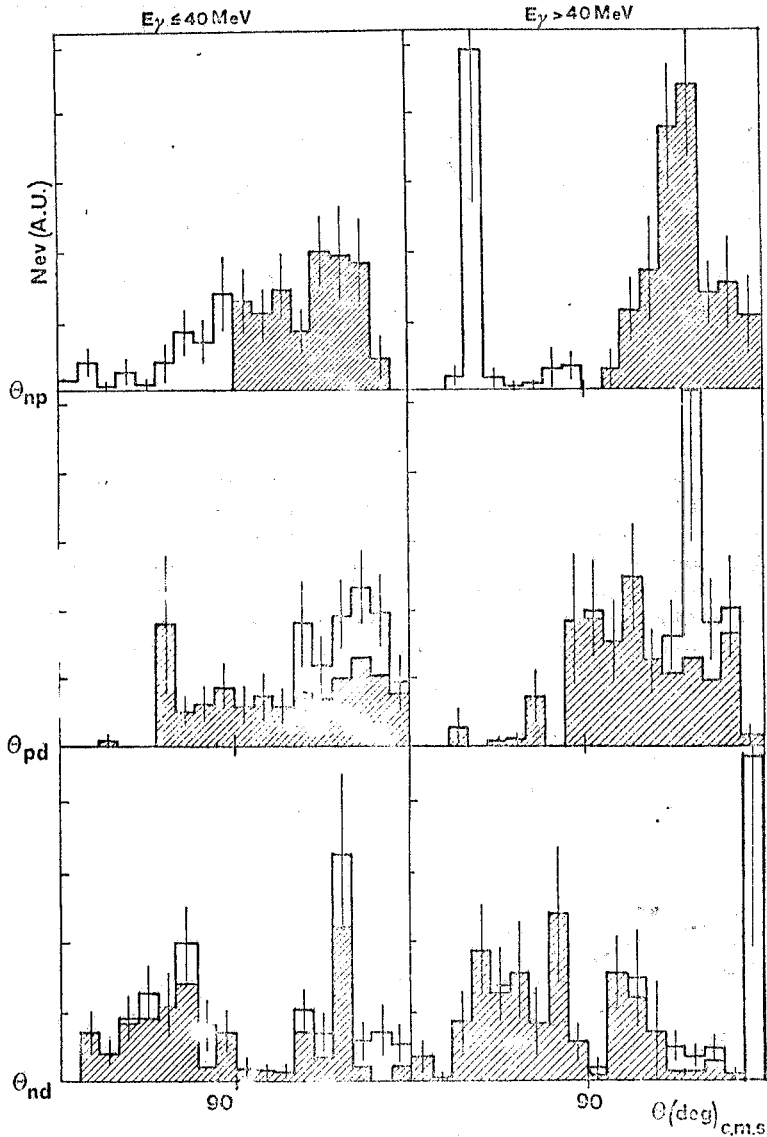


FIG. 2

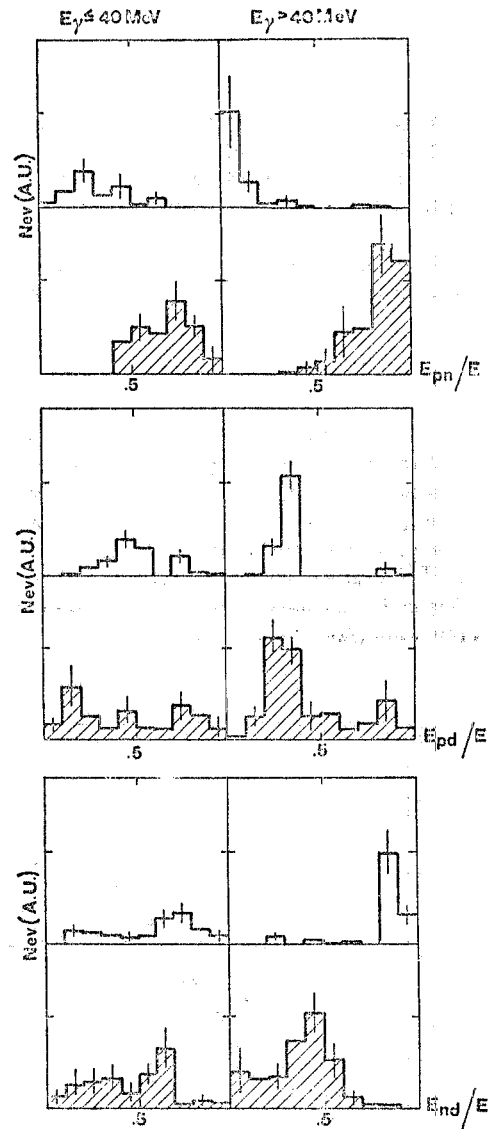


FIG. 3

FIG. 2 - Distribution of the  ${}^4\text{He}(\gamma, np){}^2\text{H}$  events as a function of the opening angle between n-p, p-d and n-d pairs. Dashed histograms: events with  $\theta_{np} > 90^\circ$ .

FIG. 3 - Distribution of the  ${}^4\text{He}(\gamma, np){}^2\text{H}$  events as a function of the relative energy of the n-p, p-d and n-d pairs, in units of their maximum possible energy  $E$ . Dashed histograms: events with  $\theta_{np} > 90^\circ$ . For  $\theta_{np} > 90^\circ$  events the n-p pairs are with the highest relative energy, for  $\theta_{np} \leq 90^\circ$  and  $E_\gamma > 40$  MeV events the n-d pairs are with the highest energy.

energies of the n-p, p-d and n-d pairs are shown. The total energy is<sup>(3)</sup>:

$$E = E_\gamma \left( 1 - \frac{E_\gamma}{2(M_4 + E_\gamma)} \right) - Q,$$

where  $E_\gamma$  is the photon energy,  $Q = (M_p + M_n + M_d) - M_4 = M_4' - M_4$  and  $M_p$ ,  $M_n$ ,  $M_d$  and  $M_4$  are the masses of the photon, neutron, deuteron and alpha respectively. The relative energy of each pair is related to the energy of the third particle. For example, in the case of n-p pair, the relative energy is<sup>(3)</sup>:

$$E_{pn}/E = 1 - E_d/E_{dmax}; \quad \text{where} \quad E_{dmax} = E(M_4' - M_d)/M_4'.$$

In particular the Fig. 3 shows that for  $\theta_{np} > 90^\circ$  (dashed histograms) the n-p pairs are with the highest relative energy and that the main mechanism, for the  $(\gamma, pn)$  reaction, is the n-p absorption of the  $\gamma$ . For the  $\theta_{np} \leq 90^\circ$  and  $E_\gamma > 40$  MeV the n-d pairs are with the highest relative energy, giving the indication that the photons are absorbed also by n-d pairs. In Table I and II the angular and energy correlation are summarized. Fig. 4 shows the cross-sections for the  $(\gamma, np)$  reaction, deduced separately for the events with  $\theta_{np} > 90^\circ$  and with  $\theta_{np} \leq 90^\circ$ . For the  $\theta_{np} > 90^\circ$  events, the cross-section is in very good agreement with the theoretical previsions of Noguchi and Prats<sup>(6)</sup>, better than in the comparison of Fig. 1. Moreover, for  $E_\gamma > 40$  MeV and  $\theta_{np} > 90^\circ$ , the  ${}^4\text{He}(\gamma, pn)$  cross-section behaviour is very similar to that of the deuteron photodisintegration cross-section<sup>(7)</sup> and also the angular distribution of protons and neutrons are similar (see Figs. 5 and 6) to those of the deuteron photodisintegration.

TABLE I

Average values of the opening angles (c. m. s.) between n-p, p-d, n-d pairs.

	$28 \leq E_\gamma \leq 40$ MeV			$40 < E_\gamma < 60$ MeV		
	$\theta_{np}$	$\theta_{pd}$	$\theta_{nd}$	$\theta_{np}$	$\theta_{pd}$	$\theta_{nd}$
$\theta_{np} \leq 90^\circ$	63°	145°	125°	40°	145°	166°
$\theta_{np} > 90^\circ$	125°	115°	85°	142°	116°	73°

TABLE II

Average values of the relative energy of the n-p, p-d, n-d pairs, related to the energy of the third particle.

	$28 \leq E_\gamma \leq 40$ MeV			$40 < E_\gamma < 60$ MeV		
	$E_{np}/E$	$E_{pd}/E$	$E_{nd}/E$	$E_{np}/E$	$E_{pd}/E$	$E_{nd}/E$
$\theta_{np} \leq 90^\circ$	0.40	0.58	0.59	0.15	0.37	0.82
$\theta_{np} > 90^\circ$	0.69	0.44	0.47	0.82	0.43	0.37

FIG. 4 -  ${}^4\text{He}(\gamma, pn){}^2\text{H}$  reaction cross-section deduced with the  $\theta_{np} > 90^\circ$  events (full line hystogram) and with the  $\theta_{np} \leq 90^\circ$  events (dashed line hystogram), compared with the calculation of ref. (6) (full line curve) and with the cross-section calculations and measurements of the photodisintegration of deuterium (7).

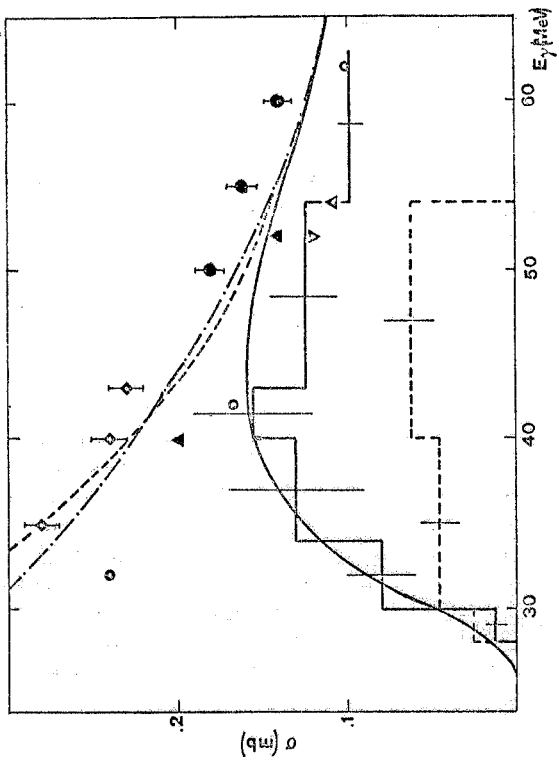


FIG. 5 and 6 - Angular distribution of p, n and d from  ${}^4\text{He}(\gamma, pn){}^2\text{H}$  reaction. Dashed hystogram: events with  $\theta_{np} > 90^\circ$ . Open circles, full points and crosses: angular distribution of n and p in the deuterium photodisintegration (7).

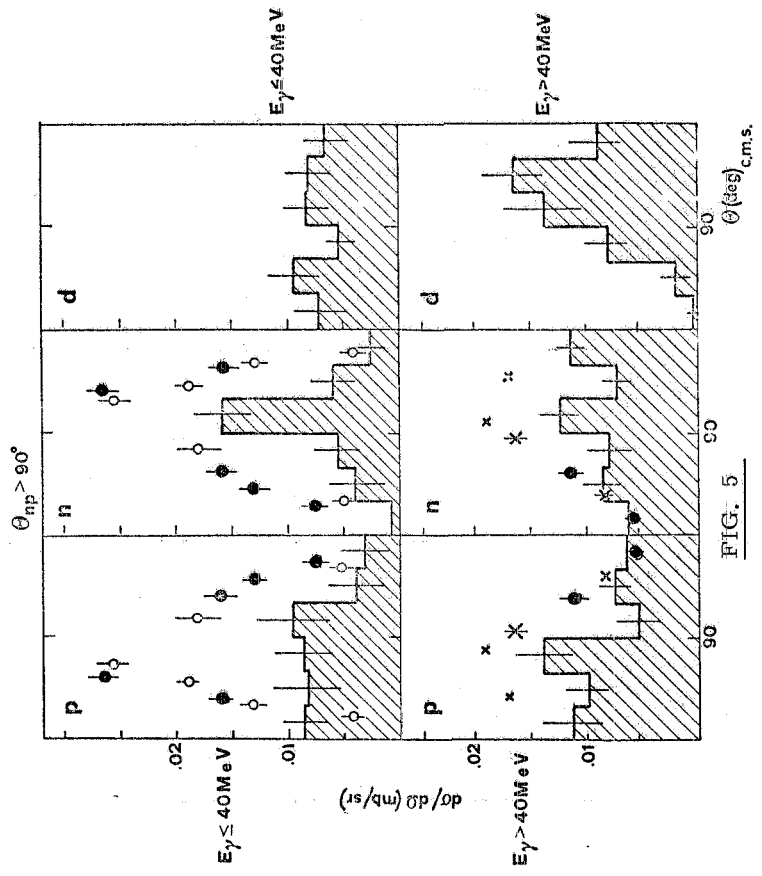


FIG. 5

FIG. 6

In Fig. 7 the cross-section of the total photodisintegration of  ${}^4\text{He}$  is shown. Our result is in rather good agreement with the older measurements of Gorbunov<sup>(3)</sup> and of Arkatov et al.<sup>(8)</sup>. Fig. 8 shows the distribution of the events as a function of the opening angle between the protons. As one can see, the protons are emitted with large relative angle suggesting the hypothesis of a unique reaction mechanism in all the energy interval investigated. The reaction mechanism can be the photoabsorption from a quasi-deuteron correlated to another quasi-deuteron, which is decomposed too.

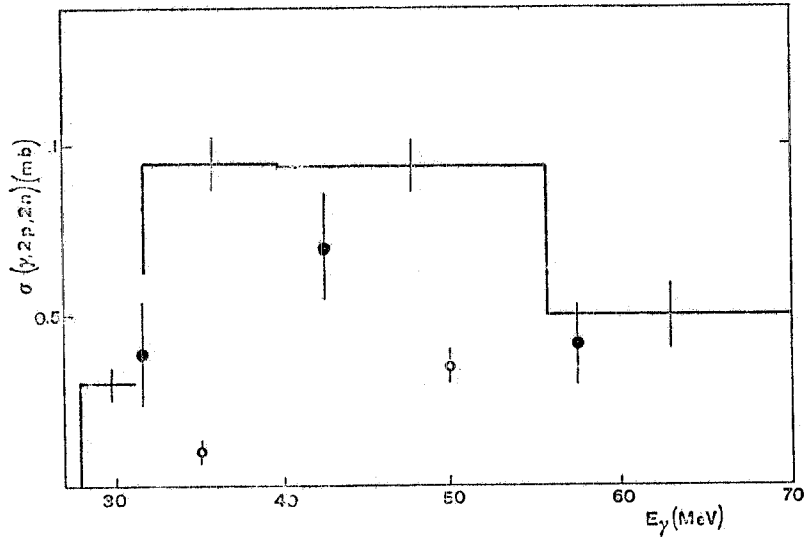


FIG. 7 -  ${}^4\text{He}(\gamma, 2p2n)$  reaction cross-section. Full line histogram: present work; full points: ref. (3); open circles: ref. (4).

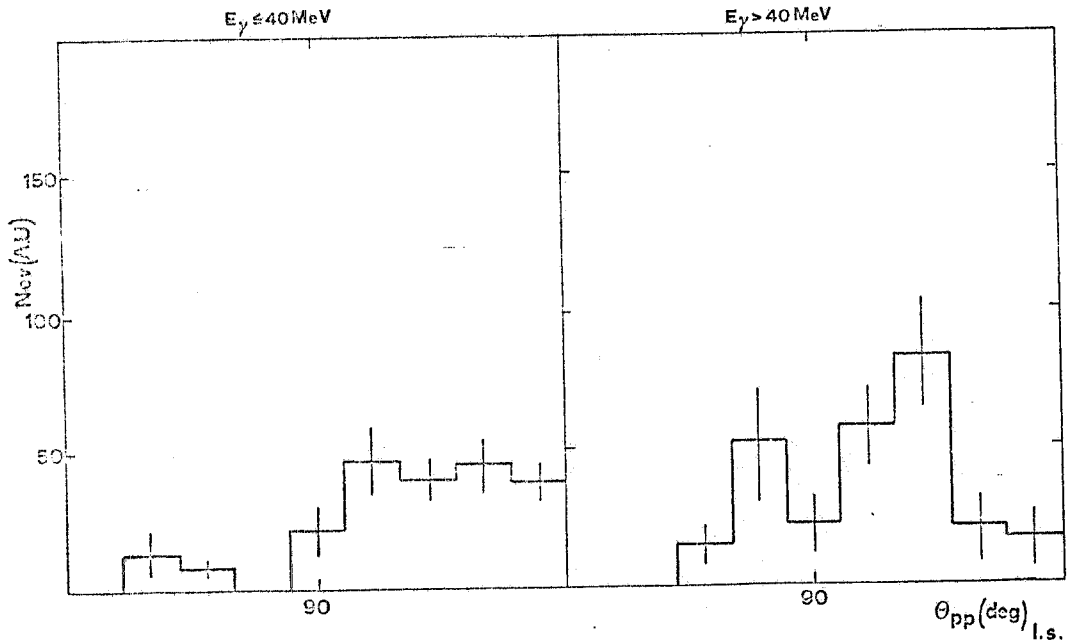


FIG. 8 - Distribution of the  ${}^4\text{He}(\gamma, 2p2n)$  events as a function of the opening angle between the protons.

With the same detector, exposed to the  $\pi^+$  beam of Frascati Laboratory<sup>(9)</sup>, we studied the non-elastic ( $\pi^+$ ,  $^4\text{He}$ ) reactions at 120, 145 and 165 MeV. The energy and angular correlations, obtained at 145 MeV, are presented. Fig. 9 shows, for the ( $\pi^+$ , 2p2n) reaction, the differential cross-section and the distribution of the events as a function of the opening angle between the protons. Both the behaviours are almost isotropic, without the strong angular correlation between the protons showed by the total photodisintegration process. In this case the total disintegration of the  $^4\text{He}$  seems to proceed via the pion multiple scattering.

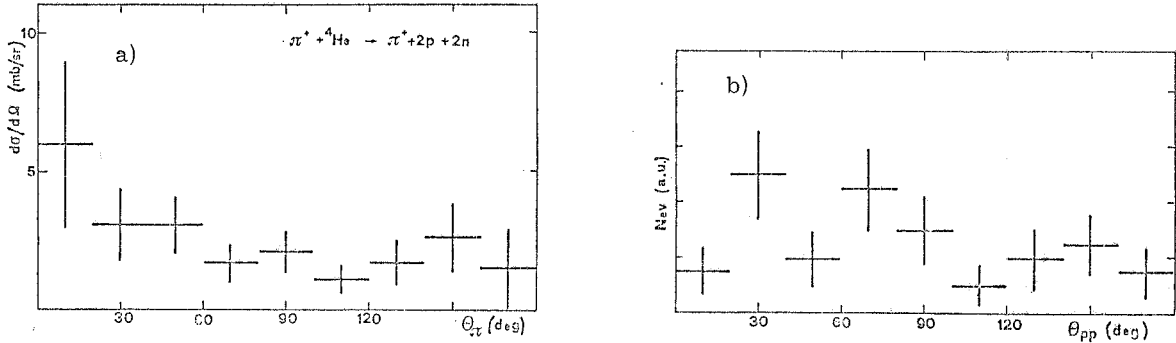


FIG. 9 - a)  $\pi^+ + ^4\text{He} \rightarrow \pi^+ + 2p + 2n$  reaction cross-section at  $E_\pi = (145 \pm 10)$  MeV; b) distribution of the events as a function of the opening angle (l. s.) between the two protons.

In the case of  $\pi^+$  absorption ( $\pi^+ + ^4\text{He} \rightarrow 3p + n$ ) reaction, the two faster protons are emitted mostly at large relative angle, as shown in Fig. 10. This angular correlation is in very good agreement with that obtained in the measurement of  $\pi^+$  absorption in nuclear emulsion<sup>(10)</sup> and with the indication of  $\pi^+$  absorption in  $^4\text{He}$  on a n-p pair, obtained by Jackson et al.<sup>(11)</sup>. Fig. 10 shows, also, that the absorption of  $\pi^+$  in  $^4\text{He}$  is similar to that of  $\pi^+$  in  $^2\text{H}$  (ref. (12)) and very different

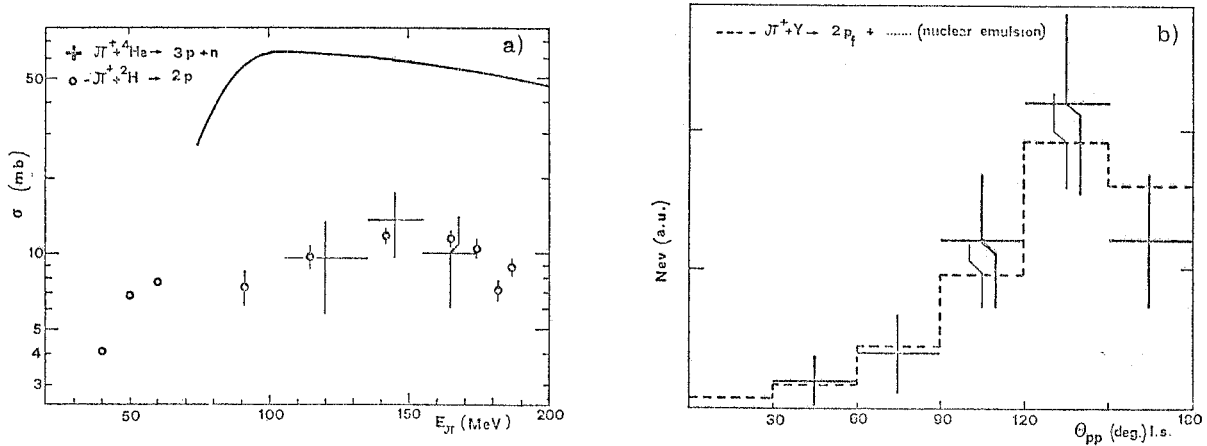


FIG. 10 - a)  $\pi^+ + ^4\text{He} \rightarrow 3p + n$  reaction cross-section at  $E_\pi = (120 \pm 15)$ ,  $(145 \pm 10)$ ,  $(165 \pm 10)$  MeV (crosses), compared with the  $\pi^+ + ^2\text{H} \rightarrow 2p$ <sup>(12, 16)</sup> reaction cross-section (open circles) and with the calculation of Hirata et al.<sup>(13)</sup> (full line curve); b) distribution of the events ( $E_\pi = 145$  MeV) as a function of the opening angle between the two "faster" protons, compared with the distribution of fast proton pairs, produced in nuclear emulsion<sup>(10)</sup> by  $\pi^+$  absorption ( $E_\pi = 45$  MeV), as a function of their opening angles. The histograms are normalized in area.

from the previsions of Hirata et al.<sup>(13)</sup>, obtained taking into account the excitation of  $\Delta$ -nuclear states in  $(\pi, {}^4\text{He})$  scattering. Fig. 11 shows the angular distribution of the third proton, it results nearly isotropic as in the case of a proton "spectator". The energy behaviour of the absorption cross-section (Fig. 12), as in the case of the cross-section for the double charge-exchange  $\pi^+ + {}^4\text{He} \rightarrow \pi^- + 4p$ , does not present a marked bump corresponding to the isobar excitation. On the other hand also the cross-section of the  $(\pi^+, 2p2n)$  reaction is almost independent<sup>(15)</sup> on the energy, in the interval we studied (120, 145, 160 MeV). Only the inelastic reaction cross-sections, which have the character of pion interaction with one nucleon, present<sup>(15)</sup> energy behaviours bump ed at about 160 MeV.

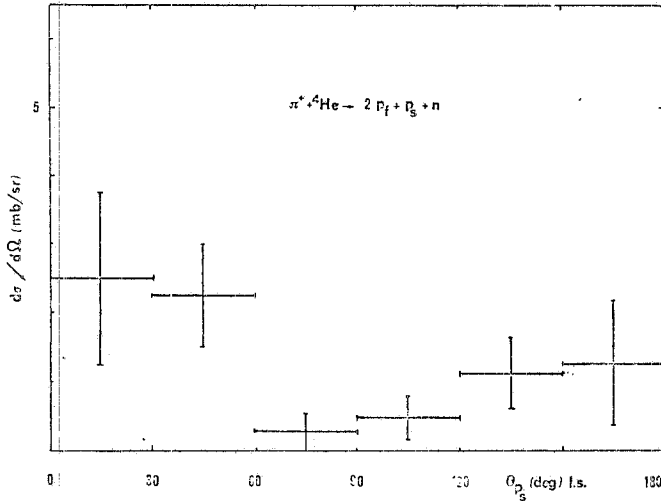


FIG. 11 - Angular distribution of the "third" proton "spectator" of the reaction  $\pi^+ + {}^4\text{He} \rightarrow 3p + n \rightarrow 2p_f + 1p_s + 1n_s$  ( $2p_f$ : two faster protons).

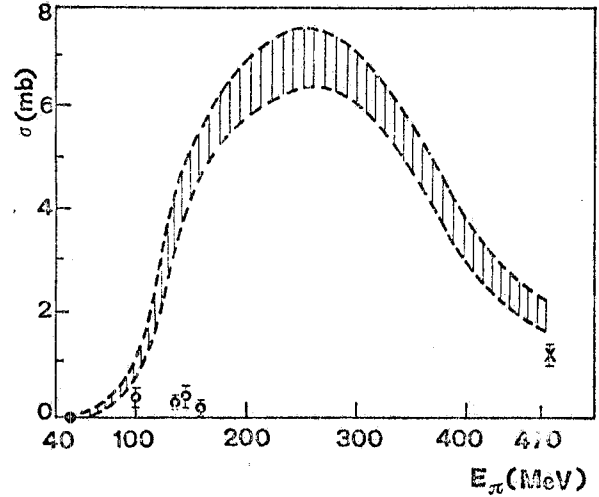


FIG. 12 - Double charge exchange cross-section  $\pi^+ + {}^4\text{He} \rightarrow \pi^- + 4p$ . Dashed line curve: prevision of the pair correlation model<sup>(14)</sup>.

Fig. 13 shows the differential cross-section of the  $(\pi^+ p {}^3\text{H})$  reaction at 145 MeV; as we can see the behaviour is very similar to that of the  $(\pi^+ p(n))$  reaction in  ${}^2\text{H}$  at 182 MeV<sup>(16)</sup> and to that of  $\pi^+$  scattering on free proton at 143 MeV<sup>(17)</sup>. Fig. 14 shows the differential cross-section of the  $(\pi^0 p {}^3\text{He})$  reaction at 145 MeV: the behaviour is similar to that of the  $(\pi^0 pp)$  reaction in  ${}^2\text{H}$ <sup>(16)</sup> and to that of  $\pi^- + p \rightarrow \pi^0 + n$  reaction<sup>(18)</sup> at 147 MeV. In the case of  $(\pi^+ n {}^3\text{He})$  reaction at 145 MeV and of  $(\pi^+ n(p))$  reaction in  ${}^2\text{H}$  at 182 MeV<sup>(16)</sup> (see Fig. 15), the differential cross-sections, in the forward angle region, are strongly higher than the cross-section for  $\pi^-$  scattering on free proton at 145 MeV<sup>(17)</sup>. The angular distributions of Fig. 16 show that, in the case of  $(\pi^+ n {}^3\text{He})$  reaction, the neutron and the  ${}^3\text{He}$  are emitted with a large relative angle, suggesting the hypothesis of a different interaction in the final state of the  $n$ - ${}^3\text{He}$  pair respect to that of the  $p$ - ${}^3\text{H}$  and  $p$ - ${}^3\text{He}$  pairs.



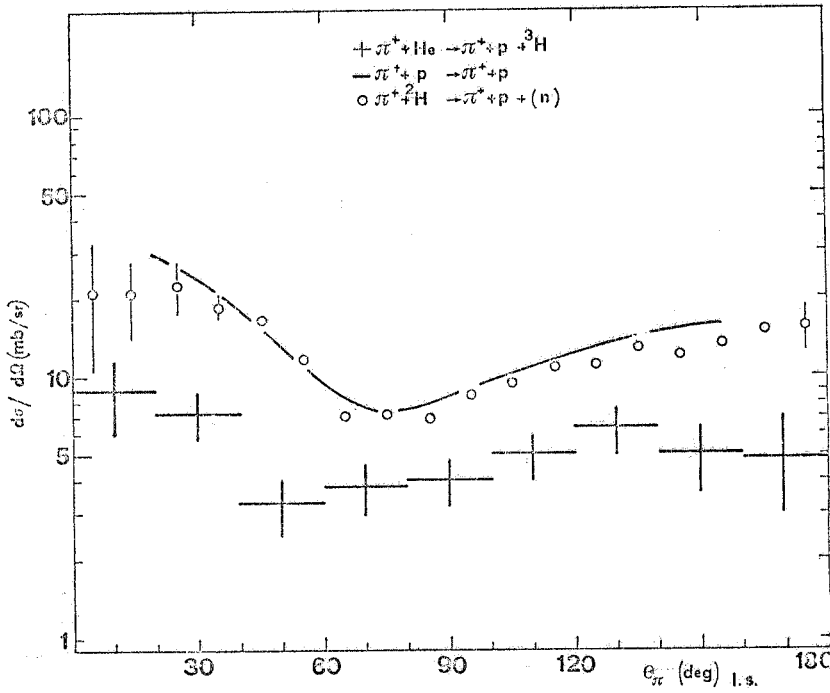


FIG. 13 - Angular distribution of  $\pi^+$  from the  $\pi^+ + {}^4\text{He} \rightarrow \pi^+ + p + {}^3\text{He}$  reaction at  $E_\pi = (145 \pm 10)$  MeV (crosses), compared with that of the  $\pi^+ + {}^2\text{He} \rightarrow \pi^+ + p + n$  reaction at  $E_\pi = 182$  MeV<sup>(16)</sup> (open circles) and with the differential cross-section of the  $\pi^+$  elastic scattering on proton at  $E_\pi = 143$  MeV<sup>(17)</sup> (full line curve).

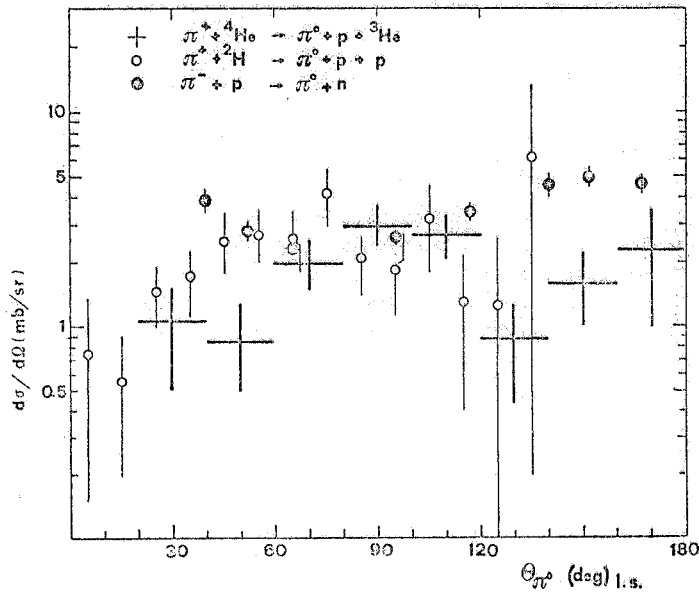


FIG. 14 - Angular distribution of  $\pi^0$  from the  $\pi^+ + {}^4\text{He} \rightarrow \pi^0 + p + {}^3\text{He}$  reaction at  $E_\pi = (145 \pm 10)$  MeV (crosses) compared with that from the  $\pi^+ + {}^2\text{H} \rightarrow \pi^0 + p + p$  reaction at  $E_\pi = 182$  MeV<sup>(16)</sup> (open circles) and with the differential cross-section of the  $\pi^- + p \rightarrow \pi^0 + n$  reaction<sup>(18)</sup> at  $E_\pi = 147$  MeV (full points).

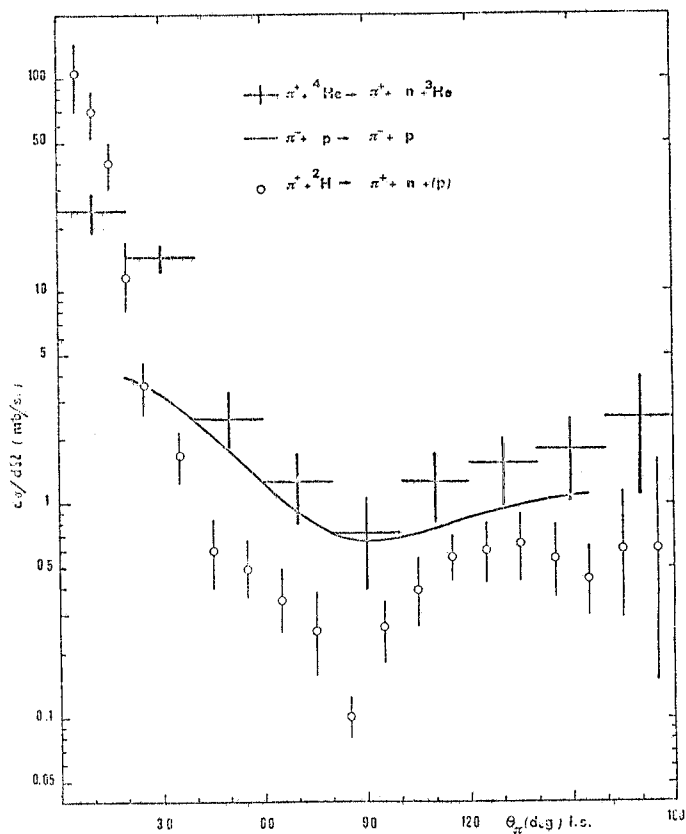


FIG. 15 - Angular distribution of  $\pi^+$  from the  $\pi^+ + {}^4\text{He} \rightarrow \pi^+ + n + {}^3\text{He}$  reaction at  $E_{\pi^+} = (145 \pm 10)$  MeV (crosses), compared with that from the  $\pi^+ + {}^2\text{H} \rightarrow \pi^+ + n + (p)$  reaction at  $E_{\pi^+} = 182$  MeV<sup>(16)</sup> (open circles) and with the differential cross-section of the  $\pi^-$  elastic scattering on proton at  $E_{\pi^-} = 144$  MeV<sup>(17)</sup>.

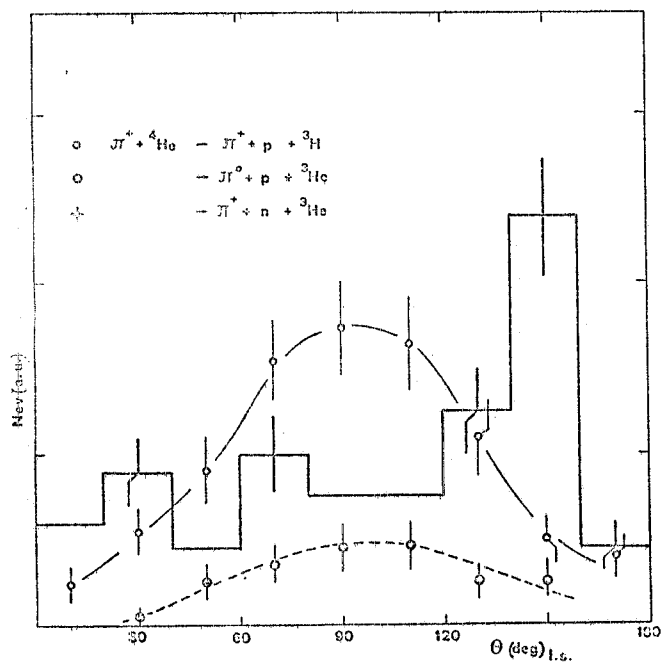


FIG. 16 - Distribution of the  $(\pi^+ p {}^3\text{H})$  (open circles),  $(\pi^0 p {}^3\text{He})$  (full points) and  $(\pi^+ n {}^3\text{He})$  (full line histogram) events as a function of the opening angle between  $p-{}^3\text{H}$ ,  $p-{}^3\text{He}$ ,  $n-{}^3\text{He}$ ,  $\bar{r}_e$  respectively. The curve lines are drawn to guide the eye.

REFERENCES. -

- (1) - R. Garfagnini et al., *Atti Accad. Sci., Torino* 102, 311 (1967).
- (2) - F. Balestra et al., *Nuovo Cimento* 38A, 145 (1977).
- (3) - A. N. Gorbunov, *Proc. of P. N. Lebedev Phys. Institute* 71, 1 (1974).
- (4) - Yu. M. Arkatov et al., *Journ. Phys.* 10, 639 (1970).
- (5) - R. I. Dzhibuti et al., *Soviet Journ. Nuclear Phys.* 7, 489 (1968).
- (6) - C. T. Noguchi and F. Prats, *Phys. Rev. Letters* 33, 168 (1974); *Phys. Rev.* 14C, 1133 (1976).
- (7) - B. Weissmann and H. L. Schultz, *Nuclear Phys.* 174A, 129 (1971); L. A. Allen, *Phys. Rev.* 98, 705 (1955); A. Galey, *Phys. Rev.* 117, 763 (1960); H. Arenhovel and W. Fabian, *Phys. Letters* 52B, 303 (1974); F. Partovi, *Ann. Phys.* 27, 79 (1964); J. J. de Swart and R. E. Marshak, *Phys. Rev.* 111, 272 (1958); Yu. A. Aleksandrov et al., *Soviet Phys. -JETP* 6, 472 (1958); B. A. Whalin, *Phys. Rev.* 95, 1362 (1954).
- (8) - Yu. A. Arkatov et al., *Soviet Nuclear Phys.* 16, 6 (1973).
- (9) - L. Busso et al., *Nuclear Instr. and Meth.* 102, 1 (1972).
- (10) - S. C. Chakravartty and J. Hebert, *Phys. Rev.* 16, 1097 (1977).
- (11) - H. E. Jackson et al., *Phys. Rev. Letters* 39, 1601 (1977).
- (12) - B. M. Freedom et al., *Phys. Rev.* 17C, 1402 (1978); C. Richard-Serre et al., *Nuclear Phys.* 20B, 413 (1970).
- (13) - M. Hirata et al., *Ann. Phys.* 108, 116 (1977).
- (14) - I. V. Falomkin et al., *Lett. Nuovo Cimento* 16, 525 (1976).
- (15) - Torino-Dubna-Frascati Collaboration, in press.
- (16) - J. H. Norem, *Nuclear Phys.* 33B, 512 (1971).
- (17) - P. J. Bussey et al., *Nuclear Phys.* 58B, 363 (1973).
- (18) - R. F. Jenefsky et al., *Nuclear Phys.* 290A, 407 (1977).